Inorganic Chemistry

Article

pubs.acs.org/IC

Rational Synthesis and Characterization of Dimolybdenum(II) Compounds Bearing Ferrocenyl-Containing Ligands toward Modulation of Electronic Coupling

Xu-Min Cai,[†] Korbinian Riener,[†] Eberhardt Herdtweck, Alexander Pöthig, and Fritz E. Kühn*

Inorganic Chemistry/Molecular Catalysis, Department of Chemistry and Catalysis Research Center, Technische Universität München (TUM), Ernst-Otto-Fischer-Straße 1, 85747 Garching bei München, Germany

Supporting Information

ABSTRACT: Three novel cis-to-trans-converted dimolybdenum(II) complexes, *trans*-[$Mo_2(O_2C$-Fc)$_2$(DPPX)$_2$][BF_4]$_2$ {**2a−2c**; DPPX = DPPA [*N*,*N*-bis(diphenylphosphino)amine], DPPM [1,1-bis(diphenylphosphino)methane], and DPPE [1,2-bis(diphenylphosphino)ethane], respectively}, were synthesized through the insertion of bulky diphosphine ligands, which force a permanent trans arrangement, as evidenced by X-ray crystallography and density functional theory calculations. All compounds were characterized by means of NMR, UV−vis, and IR spectroscopy as well as thermogravimetry−mass spectrometry measurements. Interestingly, uncommon UV−vis transitions and oxidation sequences were observed compared to previously reported ones. As verified by electrochemical measurements, all synthesized complexes show two separate one-electron-redox processes assigned to subsequent oxidations of the two redox-active ferrocenecarboxylate ligands, with a split of ca. 70 mV. This behavior reveals electronic interaction between the two equatorially trans-positioned ferrocenyl units. The presented work provides new insights into the rational synthesis of electronically coupled trans-coordinated Mo_2 systems, paving the way toward the design of linear multicenter redox-active oligomers.

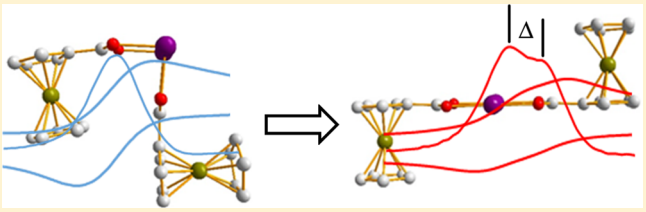

INTRODUCTION

During the last several decades, a broad variety of dimetal paddle-wheel (PW; M_2^{n+}, n = 4−6) complexes and supramolecular structures containing equatorial and axial ligands have been synthesized and characterized.[1−12] In particular, redox-active compounds with well-defined spectroscopic and electrochemical properties have attracted considerable interest in the exploration of potential applications as molecular wires and devices.[13−25] Therefore, particular attention has been paid to structural, spectroscopic, and electrochemical factors to develop novel electronic materials, e.g., molecular wires, sensors, etc.[26−44] The group of Cotton synthesized a variety of redox-active Fc-containing Mo_2 (Fc = ferrocenyl) complexes equatorially bridged by −COO units, revealing no obvious electronic coupling between cis-positioned Fc units.[34−36] Later, Ren's group published work on Fc-containing Ru_2 compounds bridged by either equatorial or axial linkers (i.e., −COO, alkynyl), executing detailed spectroscopic and electronic studies on the dimetal compounds.[37−44] On the basis of the results published so far, conclusions on electronic communication with regard to structural motifs can be drawn (Figure 1).

All compound classes in Figure 1 (1a−1e) have been studied intensively; however, they often exhibit drawbacks. Redox-active ligands axially coordinated to the dimetal unit (Figure 1a) can lead to electronic coupling ($\Delta E_{1/2}$ of ca. 300 mV) for Ru_2 motifs;[43,44] however, no communication could be observed in molybdenum systems.[26,27] From a synthetic standpoint, coordination can be weak—especially in the case of molybdenum—and also multidentate motifs cannot be employed, which limits the number of suitable ligands. For the reported dicarboxylate-linked structures (Figure 1b), electronic communication is often reported ($\Delta E_{1/2}$ of ca. 200 mV), but in this case, only the synthesis of dimers or cubelike structures has been realized, while trans coordination of one M_2 unit by two dicarboxylate ligands is not known.[2,3,34,35] For cis-coordinated, carboxylate-derived motifs (Figure 1c), electronic coupling is not very common and the synthesis toward oligomeric structures is, in general, prevented by cis coordination of the redox-active ligands.[39,40] Recent work of Chisholm's group (Figure 1d) showed electronic interactions in the trans-oriented complexes (up to 300 mV),[45,46] while previous reports on oligomers (Figure 1e) did not yield clearly defined structures.[47] This work (Figure 1f) is focused on electronic communication of trans-coordinated redox-active ligands, which might potentially result in a linear multicenter redox-active oligomer (structurally similar to Figure 1e). Recently published work of our laboratory[2] seemingly provides the ideal precursor (**1**) for the synthesis of the desired motif (Figure 1f) because it had already been reported for similar systems[48−53] that cis-ligated motifs can be transformed to trans via the insertion of bulky diphosphine ligands, leading to trans

Received: December 5, 2014
Published: March 17, 2015

DOI: 10.1021/ic502913w
Inorg. Chem. 2015, 54, 3272−3280

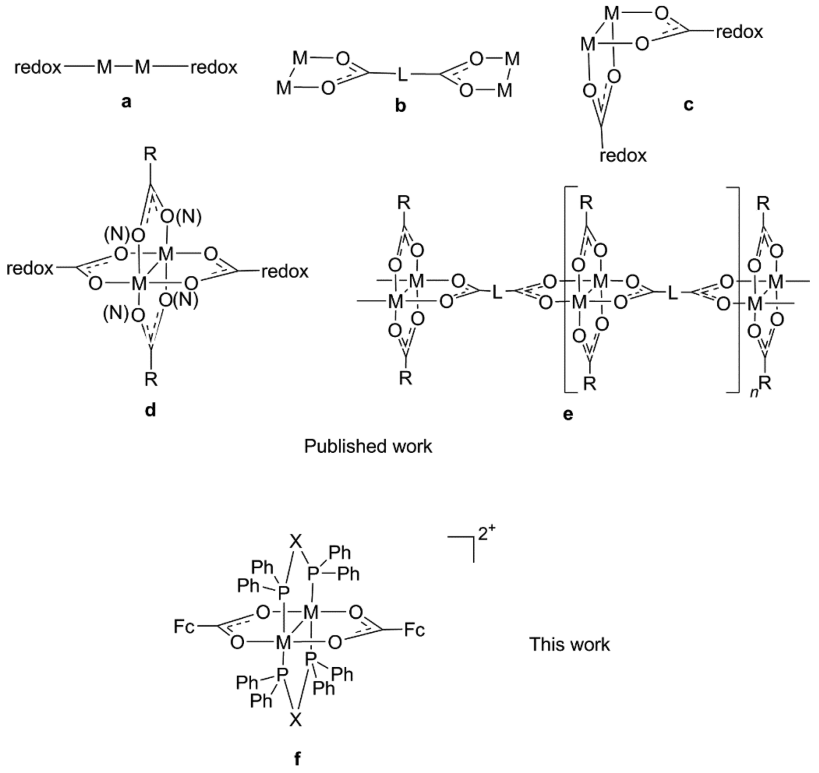

Figure 1. Overview of dimetal motifs exhibiting electronic interaction (redox = redox-active moiety; L = redox-active or organic/organometallic conjugated moiety; X = amino, methylene, or ethylene bridges; Fc = ferrocenyl).

Scheme 1. Synthesis of Compounds 2a−2c[a]

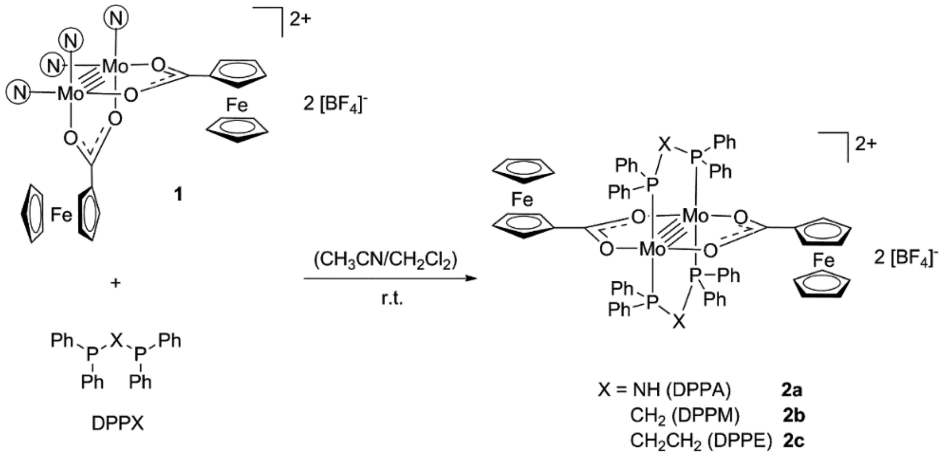

[a]Acetonitrile ligands at the Mo_2 centers are abbreviated as Ⓝ and the diphosphine ligands as DPPX.

"fixation" of the arrangement. This would be a novel example of electronic communication between two trans-coordinated carboxylate-containing ligands via a Mo_2 center. From a synthetic point of view, diphosphines seem to be advantageous as directing ligands compared to commonly used anionic bidentate ligands because the formed cationic complexes and consequently the potential oligomers are usually more soluble than neutral variants. Herein, the synthesis of three *trans*-bis(ferrocenecarboxylate)-ligated dimolybdenum(II) compounds is reported, and detailed studies of their spectroscopic and electronic properties, also including X-ray crystallographic, NMR, IR, and thermogravimetry−mass spectrometry (TG-MS) data. Density functional theory (DFT) calculations are used to underpin the experimental results on the thermodynamic stability of the presented complexes and to provide insights into their electronic structures as well as the obtained UV−vis data.

RESULTS AND DISCUSSION

Syntheses. As a supplement to the recently published work of our group,[2] the crystalline yield of *cis*-$[Mo_2(O_2C\text{-}Fc)_2(NCCH_3)_4][BF_4]_2$ (**1**) could be greatly improved up to 75% by the slow addition of 2 equiv of ferrocenecarboxylic acid to a solution of $[Mo_2(NCCH_3)_{10}][BF_4]_4$ over 2 days, followed by an additional 1 day of stirring. The key point for the synthesis is to control the dripping velocity within the first 8 h to avoid formation of the yellow side product $[Mo_2(O_2C\text{-}$

DOI: 10.1021/ic502913w
Inorg. Chem. 2015, 54, 3272−3280

Fc)$_4$].[50] Further, sufficient reaction time is necessary to avoid residuals of the trans isomer.[2] As shown in Scheme 1, compounds *trans*-[Mo_2(O_2C-Fc)$_2$(DPPX)$_2$][BF_4]$_2$ {**2a**−**2c**; DPPX = DPPA [*N*,*N*-bis(diphenylphosphino)amine], DPPM [1,1-bis(diphenylphosphino)methane], and DPPE [1,2-bis(diphenylphosphino)ethane], respectively} were prepared by reacting precursor **1** and the corresponding diphosphine ligands.

The reaction of **1** and 2 equiv of DPPA in a solvent mixture of CH_3CN and CH_2Cl_2 at room temperature affords bright-red compound **2a** in 45% crystalline yield. Both compounds **2b** and **2c** are obtained as maroon products using the same synthetic method, with 52% and 55% as crystalline yields, respectively. Full conversion of the starting materials takes place within several hours. Also, reactions of precursor **1** and 1,3-bis(diphenylphosphino)propane (DPPP) or 1,1′-bis(diphenylphosphino)ferrocene (DPPF) were attempted; however, no defined products could be obtained, as evidenced by NMR spectroscopy. This is most likely caused by the unfavored ring sizes of the metallacycles upon chelation of DPPP or DPPF to the Mo_2 center.

Thermodynamic Considerations. Because precursor **1** only exhibits one set of proton resonances for both Fc units in the ^{1}H NMR spectrum, a possible fluxional behavior in solution is assumed because the arrangement of the ferrocene ligands seen in the X-ray crystal structure would lead to multiple resonances. Therefore, a set of cis-coordinated structures were subject to DFT calculations, i.e., the Fc units facing each other, directed opposite to each other, or as illustrated in Scheme 1 (Figure S19 and Table S3 in the Supporting Information, SI). While the most stable configuration corresponds to the molecular structure observed by X-ray crystallography, the other two isomers are just about 2.5 kcal mol^{-1} higher in energy, thus providing evidence for possible fluxional behavior, which would explain the single set of proton resonances for the two Fc units. Further thermodynamic considerations seem to be reasonable with regard to the trans arrangement of the ligands in the obtained phosphine complexes. As already mentioned in the Introduction, it was intended to force trans coordination of the carboxylate units with the use of bulky phosphines. Consequently, calculations were carried out comparing the ground-state energies of the complexes with cis- versus trans-coordinated chelating diphosphine ligands. As a basis, a methylene-bridged diphosphine was subject to the study and the steric bulk of the substituents was gradually increased, from hydrogen to methyl to phenyl (Figures S20 and S21 and Table S4 in the SI). While only small energetic differences of cis and trans could be observed for R = H ($\Delta G_{cis/trans}$ = 1.1 kcal mol^{-1}), a significant increase could be observed with R = Me and Ph ($\Delta G_{cis/trans}$ = 14.6 and 23.4 kcal mol^{-1}, respectively). This trend supports the assumption that trans coordination of bulky phosphines is favored, mostly for steric reasons, therefore leading to trans-coordinated Fc units, which might further play a critical role in electronic communication.

Crystal Structure Discussion. Single crystals suitable for X-ray diffraction experiments could be obtained for all products. Crystallization of compounds **2b** and **2c** from a CH_2Cl_2 solution layered with *n*-pentane revealed trans coordination of the DPPM and DPPE ligands (Figures 2 and 3). The crystallographic data are given in Table 1, while selected bond lengths and angles together with the results of the calculations for comparison are listed in Table 2. Both

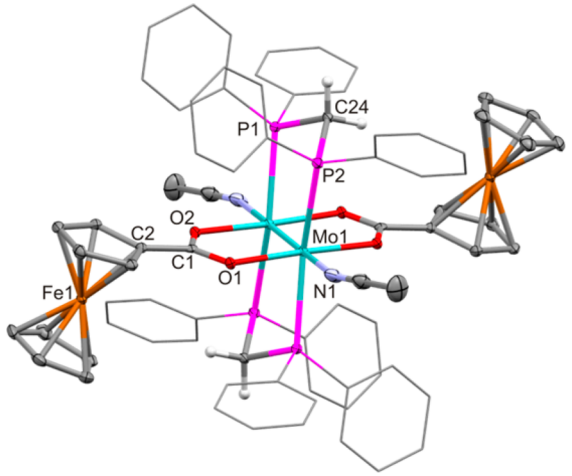

Figure 2. Molecular structure of **2b** (ellipsoids are shown at a probability level of 50%). Phenyl rings are shown as wireframes, and hydrogen atoms (except for those on the DPPM bridges) and counterions are omitted for clarity. Symmetry operation for equivalent atoms: 1 − *x*, 1 − *y*, −*z*.

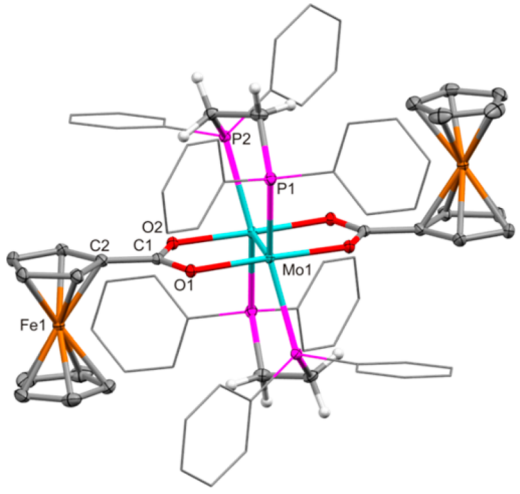

Figure 3. Molecular structure of **2c** showing one independent molecule of the asymmetric unit. Ellipsoids are shown at a probability level of 50%. Phenyl rings are shown as wireframes, and hydrogen atoms (except for those on the DPPE bridges) and counterions are omitted for clarity. Symmetry operation for equivalent atoms: 1 − *x*, 1 − *y*, 1 − *z*.

molecular structures **2b** and **2c** exhibit centers of inversion. A trans arrangement is also found in compound **2a**; however, the collected data do not allow for sufficient refinement because of the limited crystal quality (Figure S1 in the SI).

The Mo−Mo bond length of 2.1416(3) Å in compound **2b** is similar to that of 2.1315(7) Å in precursor **1**[2] and around 0.05 Å longer than that of 2.0931(2) Å in compound **2c**. Although the structures of **2b** and **2c** are similar, the bond length difference is caused by axial coordination of acetonitrile ligands in the former, which impairs the Mo−Mo bond through a bonding ($\sigma_{C\equiv N-Mo}$) and an antibonding (π_{Mo2} and $\pi^*_{N\equiv C}$) interaction. Similar comparisons can be found in the literature, with Mo−Mo bond lengths of 2.133 Å in *trans*-[Mo_2(O_2CCH$_3$)$_2$(DPPX)$_2$X$_2$]$^{2+}$ (DPPX = diphosphine ligands; X = nitriles)[50,52] and of 2.099 Å in *trans*-[Mo_2(O_2CCH$_3$)$_2$(DMPE)$_2$]$^{2+}$.[51] This can further be supported

DOI: 10.1021/ic502913w
Inorg. Chem. 2015, 54, 3272−3280

Table 1. Crystallographic Data for Compounds 2b and 2c

	2b	2c
empirical formula	$C_{76}H_{68}N_2B_2F_8Fe_2Mo_2O_4P_4$	$C_{76}H_{70}B_2Cl_4F_8Fe_2Mo_2O_4P_4$
M_r	1674.40	1790.20
cryst syst	monoclinic	triclinic
space group	$P2_1/c$	$P\bar{1}$
a (Å)	14.0024(5)	15.8736(5)
b (Å)	12.7260(4)	16.1118(5)
c (Å)	23.2277(8)	16.6044(5)
α (deg)	90	72.3049(15)
β (deg)	107.2383(16)	74.3632(16)
γ (deg)	90	70.2607(15)
V (Å^3)	3953.1(2)	3741.4(2)
Z	2	2
ρ_c (g cm^{-3})	1.407	1.589
F(000)	1696	1808
T (K)	123	123
μ(Mo Kα) (mm^{-1})	0.816	1.005
data/ restraints/ param	7243/0/452	13726/0/919
GOF (F^2)	1.075	1.027
R1[a], wR2[b] [$I > 2\sigma(I)$]	0.0438, 0.1125	0.0245, 0.0594

[a] $R1 = \sum(||F_o| - |F_c||)/\sum|F_o|$. [b] $wR2 = \{\sum[w(F_o^2 - F_c^2)^2]/\sum[w(F_o^2)^2]\}^{1/2}$.

by DFT calculations, where the calculated δ_{Mo-Mo} of 2.1097 Å in $\mathbf{2b}_{cal}$ is similar to that of 2.0931(2) Å in **2c**. All of the other parameters are quite close to the computational results, indicating that the axial acetonitriles mainly affect the Mo−Mo bond length. The remaining data of **2b** and **2c** are very alike, as expected, because of their structural similarities. Both the edge−edge distances between two Fc centers $C_\omega\cdots C_\omega'$ (C_ω and C_ω' denote the Cp carbon atoms covalently bonded to the −COO unit) of 8.35 and 8.33 Å and the Fe···Fe′ distances of 11.69 and 11.18 Å in compounds **2b** and **2c**, respectively, are much longer than those of 5.66 and 7.25 Å in **1**, which will be further discussed as part of the electrochemical studies. Both O−Mo−O angles of 177.11(9) and 176.34 (6)° for compounds **2b** and **2c** illustrate the linear trans arrangement of the $FcCOO^-$ moieties. Variation of the P1−Mo1−P2 angles for **2b** [161.893(1)°] and **2c** [142.804(2)°] can be attributed to the different ring sizes of the phosphametallacycles, i.e., five- versus six-membered rings. With regard to the Fc units, the Cp rings in all compounds are nearly eclipsed.

NMR Spectroscopy. Complexes **2a**−**2c** are diamagnetic and therefore suitable for NMR spectroscopic investigations in CD_3CN (Figures S2−S7 in the SI). Via 2D NMR measurements, the respective resonances can be assigned for further comparison (Figures S8−S10 and Table S1 in the SI), with atoms labeled in Figure S11 in the SI. In compound **2a**, the protons on the unsubstituted Cp ring (H_c/C_c) can be assigned to the shift at 3.75 ppm, which corresponds to the carbon resonance at 70.35 ppm via HSQC. Further, the signal of C_ω can be assigned to 75.13 ppm because of the absence of a direct proton correlation. For the remaining two sets of protons/carbons (H_a/C_a next to C_ω and H_b/C_b for the other pair) on the substituted Cp ring, both HSQC and HMBC are needed for interpretation. The shifts of H_a/C_a correspond to 4.65/72.63 ppm, while the ones of H_b/C_b can be attributed to 4.78/71.79 ppm because an indirect correlation of H_a to C_ω can be observed in HMBC. It seems reasonable to compare all proton signals on the ferrocene rings in compounds **2a**−**2c** to those in *trans*-$[Mo_2(O_2C\text{-}Fc)_2(NCCH_3)_4][BF_4]_2^2$ (*trans*-**1**). In the ^1H NMR spectrum of **2a**, both H_a (4.65 ppm) and H_b (4.78 ppm) are upfield-shifted by 0.14 and 0.42 ppm, respectively, compared to *trans*-**1** (4.79 and 5.20 ppm). This can be explained by the increase of the electron density caused by coordination of the donating phosphine ligands.[50] However, the large upfield shift of 0.71 ppm from H_c cannot only be an electron-donating effect; the same applies to compound **2c**. When looking at the structure of **2c**, the unsubstituted Cp ring sits between two phenyl rings (Figure 3), which is therefore affected by the aromatic ring current. In contrast to that, compound **2b** shows a reverse signal shift trend, with downfield shifts of 0.09 and 0.06 ppm on H_a and H_b, respectively, which is in accordance with the literature data.[53] The amine proton signal in compound **2a** occurs at 6.35 ppm as a triplet derived from the coupling of two adjacent phosphorus atoms. It is highly downfield-shifted about 2.04 ppm compared to the free ligand DPPA (NH, t, 4.31 ppm). Additionally, the proton signals on the phenyl rings are also slightly downfield-shifted. The only singlet at −1.17 ppm in the ^{11}B NMR spectrum and the two singlets at −151.6 and −151.7 ppm in the ^{19}F NMR

Table 2. Selected Bond Lengths (Å) and Angles (deg) for Compounds 2b and 2c

	2b[b]	$2b_{cal}$[c]	2c[c]	$2c_{cal}$[c]
Mo1−Mo1	2.1416(3)	2.1097	2.0931(2)	2.1191
Mo1−O1	2.106(2)	2.0902	2.089(2)	2.0914
Mo1−O2	2.092(2)	2.0884	2.072(2)	2.0884
Mo1−P1	2.5654(9)	2.6077	2.5987(5)	2.6341
Mo1−P2	2.597(1)	2.6376	2.5574(4)	2.6024
C1−O1	1.272(4)	1.2836	1.282(2)	1.2853
C1−O2	1.285(5)	1.2895	1.285(3)	1.2857
C1−C2	1.459(6)	1.4578	1.449(3)	1.4583
Fe···Fe′	11.6856(8)	11.7387	11.1768(6)	11.6924
$C_\omega\cdots C_\omega'$[a]	8.348(6)	8.3763	8.325(3)	8.3800
P1−Mo1−P2	161.89(3)	157.855	142.80(2)	142.271
O1−Mo1−O2	177.11(9)	176.942	176.34(6)	177.211
Fe1−C2−C2−Fe1	180.0(2)	180.000	180.0(1)	179.987

[a] C_ω and C_ω' denote Cp carbon atoms covalently bonded to the −COO unit. [b] With axial acetonitrile ligands. [c] Without axial acetonitrile ligands.

DOI: 10.1021/ic502913w
Inorg. Chem. 2015, 54, 3272−3280

spectrum confirm the presence of free BF_4^- anions. The resonance in the ^{31}P NMR can be observed at 78.45 ppm because of electron donation of DPPA (43.20 ppm, vide supra). All signals of the bridging protons and phosphorus atoms in compounds **2b** and **2c** show the same trends as those in **2a**. Interestingly, a pseudopentet at 4.34 ppm confirms that the two protons of the bridging $-CH_2-$ group are diastereotopic. The signal can be interpreted as a doublet (coupling with a neighboring proton) of triplets (two neighboring phosphorus atoms), which results in an integral ratio of 1:2:2:2:1. Identical ^1H and ^{31}P NMR spectra at room temperature and −10 °C indicate that any fluxional process cannot be significantly restricted within this temperature range, while this is the case for $[(CH_3CN)_4Mo_2(O_2C\text{-}Fc\text{-}CO_2)(BF_4)_2]_4$.[2] Further, compared to compounds **2a** and **2b**, the proton signals of the phenyl moieties in **2c** are more distinctly separated at 7.58, 7.47, and 7.33 ppm, respectively.

Electronic Structure. The calculated electronic structures of compounds **1** and **2a**−**2c** are summarized in a frontier molecular orbital diagram (Figure 4) with representations of

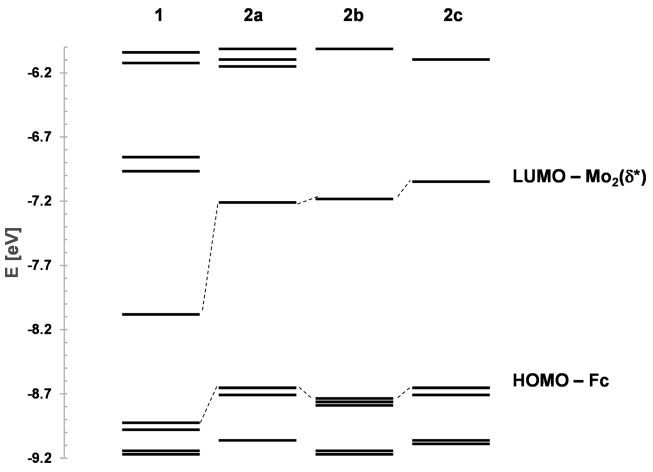

Figure 4. Frontier molecular orbital diagram of **1** and **2a**−**2c**. For further details, see the SI.

the highest occupied molecular orbital (HOMO) and lowest unoccupied molecular orbital (LUMO) of **1** (Figure 5) and **2a**

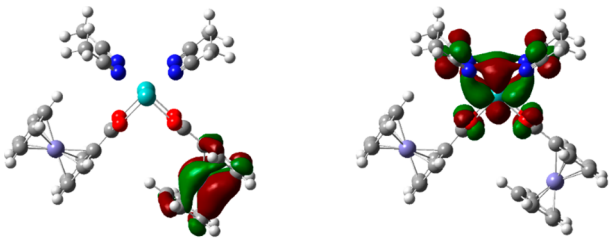

a) HOMO, Fc **b) LUMO, $Mo_2(\delta^*)$**

Figure 5. HOMO and LUMO of **1**.

(Figure 7, exemplarily for all phosphinated complexes). The three HOMOs (namely, HOMO, HOMO−1, and HOMO−2) are Fc-centered, while the LUMOs are of predominantly $Mo_2(\delta^*)$ character with some carboxylate mixing, and for **1**, also some contributions from the acetonitrile ligands can be observed.

UV−Vis Spectroscopy. The UV−vis absorption spectra of compounds **1** and **2a**−**2c** in the visible range are shown in Figure 6.

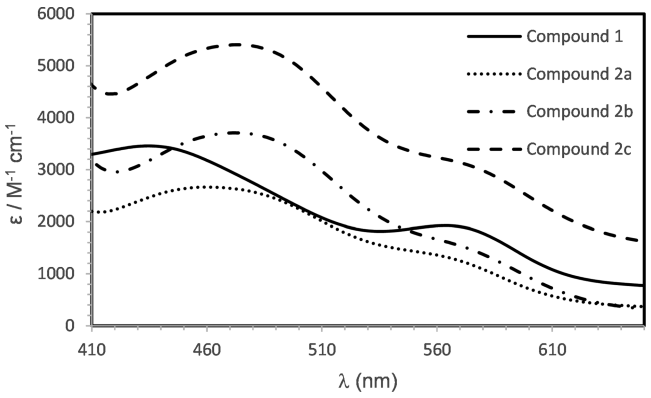

Figure 6. Visible absorption spectra of compounds **1** and **2a**−**2c** in CH_3CN (selected range). For further details, see the SI.

The absorption of **2a** at 459 nm is red-shifted about 25 nm compared to that in precursor **1**, while the absorption at 573 nm is only slightly red-shifted. The roughly similar absorptions of precursor **1** and products **2a**−**2c** in the visible range are in accordance with the color red (see the SI). Time-dependent DFT (TD-DFT) calculations were performed to provide insight into the observed absorptions. For products **2a**−**2c**, the calculated results are in good accordance with the experimental data (Table 3). The obtained data for precursor **1** matches a little less, most likely because of the fluxional behavior of the coordinated Fc ligand (vide supra).

In the literature, the characteristic absorbance of Mo_2 complexes is reported as a $\delta \rightarrow \delta^*$ transition in the region of 400−500 nm.[8,50,53] More precise assignments for Mo_2 systems were recently published using computational methods.[13,15,18,49,51] According to these publications, the low-energy absorption at around 500 nm can be assigned to a metal-to-ligand charge-transfer transition. With regard to these results, the here reported electronic structure seems to be quite different because the HOMO is uncommonly localized on the ligand (Fc).

For compound **2a** (Figure 7), the experimental absorption at about 459 nm corresponds to the calculated absorption of 484 nm, deriving mainly from the contribution of HOMO → LUMO+7. This is a transition from an Fc-based to a carboxylate-based orbital with a little mixing of Cp and the iron center, thus being a ligand-to-ligand transition with respect to the Mo_2 unit. The absorption at 573 nm is in accordance with the calculated 585 nm as a $Mo_2(\delta)$, with a minor Cp and iron contribution, to a $Mo_2(\delta^*)$ transition (HOMO−6 → LUMO). In general, these transitions are metal-to-metal transitions.

Electrochemical Properties. Electrochemical studies have often been applied to evaluate the electronic communication between distal redox-active entities.[17,34,35,44] Therefore, differential pulse voltammetry (DPV) of compounds **1** and **2a**−**2c** was performed in degassed CH_3CN, and the results are illustrated in Figure 8 and Table 4, along with cyclic voltammetry (CV) in Figure S14 in the SI.

Some electrochemical studies on the dimolybdenum system of Cotton's group have been presented during the last few decades, and it was shown that the $[Mo_2]^{4+}$ units in

DOI: 10.1021/ic502913w
Inorg. Chem. 2015, 54, 3272−3280

Table 3. Experimentally Obtained and Calculated Absorptions (Assignment of HOMO: #174 for 1, #332 for 2a/2b, and #340 for 2c)

compd	λ_{exp} (nm)	ε_{exp} (M^{-1} cm^{-1})	λ_{cal} (nm)	oscillator strength	orbital excitation	contrib (%)
1	435	3460	410	0.0126	171 → 181	66
					173 → 184	12
	564	1930	492	0.0269	171 → 180	50
					171 → 184	17
					171 → 195	20
					172 → 192	15
			502	0.0351	170 → 181	17
					173 → 181	51
					173 → 184	21
					173 → 186	17
2a	459	2670	484	0.0431	329 → 342	21
					329 → 344	23
					329 → 363	16
					330 → 340	28
					332 → 340	37
					332 → 361	11
	573	1210	585	0.0118	326 → 333	69
2b	472	3710	486	0.0461	327 → 342	12
					329 → 344	15
					330 → 338	19
					330 → 356	10
					331 → 357	13
					332 → 338	39
					332 → 359	16
	581	1350	577	0.0124	326 → 333	69
2c	473	5400	483	0.0390	335 → 350	12
					336 → 346	11
					337 → 350	26
					337 → 368	14
					339 → 365	11
					340 → 346	39
					340 → 367	13
	576	3050	588	0.0171	334 → 341	67
					340 → 342	13

dimolybdenum formamidinate complexes can undergo a one-electron-oxidation process at a potential of around 0.5 V under measurement conditions similar to those described here.[16,24,34,35] $[Mo_2(NCMe)_{10}][BF_4]_4$, which is used for the synthesis of **1**, only exhibits one irreversible oxidation peak of the $[Mo_2]^{4+}$ unit at a potential of about 2.1 V, derived from the electron-deficient $[Mo_2]^{4+}$ center weakly coordinated by 10 acetonitrile molecules. The reversible oxidation peak of the Fc unit at around 0.91 V in Fc−COOH, as well as the published cis precursor complex **1** from our group, was measured for comparison. Table 4 contains all of the obtained electrochemical data. On their basis, the following conclusions can be drawn (Scheme 2): (i) The first oxidation E^1 can be assigned to a Fc-centered process, contrasting the situation observed for Cotton's complexes,[34,35] where the $[Mo_2]^{4+}$ core is oxidized first. (ii) The second oxidation E^2 is ascribed to a further Fc-centered redox step, with the split of the first two oxidation peaks of about 70 mV in all products (**2a**−**2c**), indicating electronic interaction between the two Fc units, while such splitting cannot be observed in precursor **1**. (iii) The irreversible oxidation couple E^3 is assigned to $[Mo_2]^{4+}/[Mo_2]^{5+}$ at around 1.9 V and is more than 400 mV positively

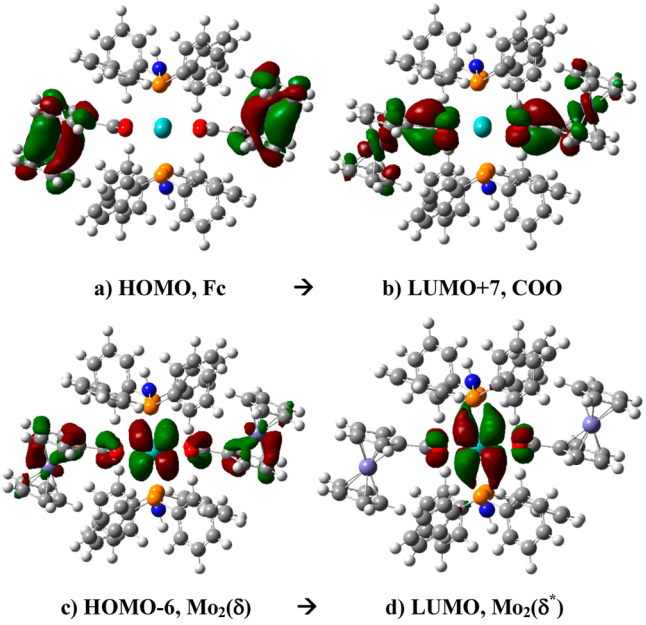

Figure 7. Main contributing transitions exemplified for compound **2a** (top, 484 nm; bottom, 585 nm).

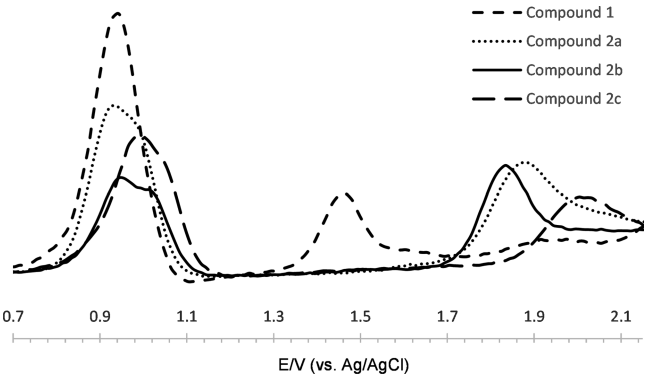

Figure 8. DPV of compounds **1** and **2a**−**2c**. The results were recorded in a 0.10 M degassed CH_3CN solution of $[Bu_4N][BF_4]$.

Table 4. Electrochemical Data (in V) for All Compounds

compd	$E_{1/2}$ (E^1) for Fc^0/Fc^+	$E_{1/2}$ (E^2) for Fc^+/Fc^{2+}	$E_{1/2}$ for Fc^0/Fc^{2+}	$\Delta E_{1/2}$[a] (mV)	$E_{1/2}$ (E^3) for Mo_2^{4+}/Mo_2^{5+}
FMCA	0.91				
$[Mo_2(NCMe)_{10}][BF_4]_4$					2.10
1			0.94		1.47
2a	0.92	0.99		70	1.89
2b	0.95	1.02		70	1.86
2c	0.99	1.05		60	2.03

[a]Calculated from the difference between $E_{1/2}(Fc^+/Fc^{2+})$ and $E_{1/2}(Fc^0/Fc^+)$.

Scheme 2. Assignment of the Step-by-Step Redox Processes

$$[Fc^{II}Mo_2^{IV}Fc^{II}]^{2+} \overset{E^1,\ -e^-}{\rightleftharpoons} [Fc^{III}Mo_2^{IV}Fc^{II}]^{3+} \overset{E^2,\ -e^-}{\rightleftharpoons} [Fc^{III}Mo_2^{IV}Fc^{III}]^{4+} \overset{E^3,\ -e^-}{\rightleftharpoons} [Fc^{III}Mo_2^{V}Fc^{III}]^{5+}$$

shifted, compared to compound **1**. This can be explained by stabilization through the electronically coupled trans-coordinated Fc centers in **2a**−**2c**, which can also be seen in the DPV

DOI: 10.1021/ic502913w
Inorg. Chem. 2015, 54, 3272−3280

spectrum of a *cis*- and *trans*-**1** mixture (Figure S15 in the SI). According to the spectroscopic results, both Fc oxidations of the mixture overlap, while a distinct difference of the $[Mo_2]^{4+}/[Mo_2]^{5+}$ oxidations can be found with *trans*-**1** (1.76 V), around 300 mV higher compared to that of *cis*-**1**.

It is mentioned in the literature that the weak electronic communication in compounds *cis*-$[Ru_2(D(3,5\text{-}Cl_2Ph)F)_2(O_2C\text{-}Fc)_2Cl]$ and *cis*-$[Ru_2(DmAmiF)_2(O_2C\text{-}Fc)_2Cl]$ [D(3,5-Cl_2Ph)F = *N*,*N*′-di(3,5-dichlorophenyl)formamidinate; DmAmiF = *N*,*N*′-di(3-methoxyphenyl)formamidinate] is either enabled through space or due to the covalent linkage.[39,40] Because no electronic interaction could be found in Fc-containing cis precursor **1**, it appears rational to propose that electronic coupling is achieved by electronic delocalization through covalent linkage separated by six bonds in all trans products.

In order to get experimental data on the oxidized species, chemical oxidation was attempted using established reagents such as $AgBF_4$ and $NOBF_4$. However, none of them yielded the desired products. While $AgBF_4$ led to phosphine decoordination, for $NOBF_4$ no defined products could be isolated.

CONCLUSIONS

Novel dimolybdenum complexes **2a**−**2c** bearing bidentate trans-coordinated ferrocenecarboxylate ligands can be prepared by reacting **1** with bulky diphosphine ligands. The synthetic route used the steric demand of the employed phosphines to transfer cis-coordinated precursor **1** to a trans arrangement in the obtained products. Most of the structures could be unambiguously assigned via X-ray crystallography. Further characterization techniques included NMR and IR spectroscopy as well as TG−MS, UV−vis spectroscopy in combination with computational data points toward uncommon electronic transitions. In addition, electrochemical measurements revealed electronic communication of the redox-active ferrocene-derived ligands in all obtained products. Interestingly, the oxidation sequence is different from all similarly reported systems.

All in all, the presented work provides valuable insights into the rational synthesis of electronically coupled Mo_2 systems, paving the way toward the design of linear multicenter redox-active oligomers. Therefore, a reverse synthetic strategy is currently being established, namely, the reaction of a Mo_2 precursor, bearing two trans-coordinated diphosphine and further labile ligands, with redox-active dicarboxylate linkers.

EXPERIMENTAL SECTION

General Procedure and Materials. All preparations and reactions were carried out under argon using standard Schlenk techniques. All solvents were dried using standard procedures.[54] All diphosphine ligands were purchased from ABCR (*N*,*N*-bis(diphenylphosphino)amine, 98%; 1,1-bis(diphenylphosphino)methane, 99%; 1,2-bis(diphenylphosphino)ethane, 97%) and used as received. Precursor **1** was prepared according to a literature procedure[2] and is in this paper referred to by the formula $[Mo_2(O_2C\text{-}Fc)_2(NCCH_3)_4][BF_4]_2$ after overnight drying. NMR measurements were performed on Bruker AVANCE-DPX-400 and Avance-DRX-400 MHz spectrometers (^{1}H, 400.13 MHz; ^{11}B, 128.38 MHz; ^{13}C, 100.61 MHz; ^{19}F, 376.50 MHz; ^{31}P, 161.97 MHz). Chemical shifts were reported in ppm and referenced to the solvent as an internal standard. IR spectra were recorded on a Varian FTIR-670 spectrometer, using a GladiATR accessory with a diamond ATR element. Elemental analyses were carried out at the microanalytical laboratory of TUM. UV−vis spectra were recorded with a Jasco V-550 spectrophotometer. Solution spectra were measured in a quartz cell with a 1 cm path length (background: solvent vs solvent). Electrospray ionization mass spectrometry (ESI-MS) spectra were recorded on a ThermoElectron LCQ classic, with 0.10% formic acid/water as a buffer. Thermogravimetric analysis in combination with online fragment detection via coupled mass spectrometry (TG−MS) was conducted utilizing a Netzsch-STA 409 PC/PG; typically about 3 mg of each sample was heated from 30 to 1000 °C at 10 °C min^{-1}. CV and DPV were recorded in a 0.10 M $[Bu_4N][BF_4]$ solution (CH_3CN, degassed) on a Gamry Reference 600 voltammetric analyzer with a Pt working electrode (diameter = 1 mm), a Pt/Ti wire auxiliary electrode, and a Ag/AgCl reference electrode. The concentration of all of the samples was 7.0 mM. All of the potential values are referenced to Ag/AgCl, and under the present experimental conditions, $E_{1/2}$[ferrocene(0)/ferrocene(+)] was consistently measured at 0.64 V.

DFT Calculations. All calculations used DFT methodology, as implemented in the *Gaussian09* package[55] using the hybrid O3LYP functional[56,57] with the SDD basis set employed for molybdenum, aug-CC-pvDZ for oxygen, and standard 6-31G*[58,59] for the remaining atoms. No symmetry or internal coordinate constraints were applied during optimizations. Calculated structures were verified as being true minima by the absence of negative eigenvalues in the vibrational frequency analysis. For the TD-DFT calculations, 60 singlet excitations for the respective compounds were obtained.[16] Detailed computational data are provided in the SI.

*Improved Synthesis of cis-$[Mo_2(O_2C\text{-}Fc)_2(NCCH_3)_4][BF_4]_2$ (**1**).* A blue solution of 1 equiv of $[Mo_2(NCCH_3)_{10}][BF_4]_4$ (380 mg, 400 μmol) in 40 mL of CH_3CN was stirred, and 2 equiv of ferrocenemonocarboxylic acid (184 mg, 800 μmol) in 60 mL of tetrahydrofuran was slowly added over 8 h. The reaction mixture was stirred for 3 days at 55 °C to yield a red solution. After filtration, the solvents were evaporated under reduced pressure. The obtained red solid was ultrasonically washed in CH_2Cl_2 several times and redissolved in 12 mL of CH_3CN and 10 mL of CH_2Cl_2, followed by layering with 24 mL of *n*-pentane. Crystalline compound **1** was obtained in 1 week with a yield of 75%. All characterization data match those in the previously published paper.[2] DPV: Fc^0/Fc^{2+}, 0.94 V; Mo_2^{4+}/Mo_2^{5+}, 1.47 V.

*Synthesis of trans-$[Mo_2(O_2C\text{-}Fc)_2(DPPA)_2][BF_4]_2$ (**2a**).* A solution of 1 equiv of **1** (197 mg, 200 μmol) and 2 equiv of bis(diphenylphosphino)amine (154 mg, 400 μmol) in a solvent mixture of CH_3CN (10 mL) and CH_2Cl_2 (10 mL) was stirred overnight at room temperature to yield a dark-red solution, which was dried under reduced pressure. The obtained dark-red solid was redissolved in 10 mL of CH_2Cl_2 and layered with 10 mL of *n*-pentane. Small bright-red, air- and moisture-sensitive crystals formed overnight. The red crystals were collected, washed several times with diethyl ether and *n*-pentane, and dried under vacuo. Compound **2a** was obtained in a yield of 45%. ^{1}H NMR (CD_3CN): δ 7.40−7.60 (m, 40H, H_{ph}), 6.33 (t, 2H, NH), 4.78 (t, 4H, H_{cp}), 4.65 (t, 4H, H_{cp}), 3.75 (s, 10H, H_{cp}). ^{11}B NMR (CD_3CN): δ −1.17 (s, BF_4^-). ^{13}C NMR (CD_3CN): δ 191.4 (COO^-), 134.5 (m, C_{ph}), 132.9 (m, C_{ph}), 130.0 (m, C_{ph}), 75.13 ($C_{quart\text{-}cp}$), 72.63 (C_{cp}), 71.79 (C_{cp}), 70.35 (C_{cp}). ^{19}F NMR (CD_3CN): δ −151.60 (s, BF_4^-), −151.65 (s, BF_4^-). ^{31}P NMR (CD_3CN): δ 78.45. Anal. Calcd for $(C_{70}H_{60}B_2F_8Fe_2Mo_2N_2O_4P_4)$ = $[Mo_2(O_2C\text{-}Fc)_2(DPPA)_2][BF_4]_2$: C, 52.73; H, 3.79; N, 1.76; P, 7.77. Found: C, 52.31; H, 3.91; N, 1.98; P, 7.64. Selected IR (cm^{-1}): ν(NH) 3238w, ν_a(COO) 1491m, ν_s(COO) 1390m, ν(BF) 1098m. ESI-MS (*m*/*z*): $[DPPA + H]^+$, 386.3 (calcd 386.1); $[(M - 2BF_4)/2]^+$, 710.3, 710.9, 711.6 (calcd 710.0, 710.5, 711.0); $[M - DPPA - 2BF_4 + HCOO]^+$, 1078.9, 1079.9, 1080.9, 1081.9 (calcd 1077.9, 1079.9, 1080.9, 1081.9).

*Synthesis of trans-$[Mo_2(O_2C\text{-}Fc)_2(DPPM)_2][BF_4]_2$ (**2b**) and trans-$[Mo_2(O_2C\text{-}Fc)_2(DPPE)_2][BF_4]_2$ (**2c**).* **2b** and **2c** were obtained with the same synthetic procedure as that for **2a** by using DPPM and DPPE instead of DPPA, respectively. Dark-red, air- and moisture-sensitive crystals of **2b** as well as maroon crystals of **2c** formed quickly overnight and were suitable for X-ray crystallographic measurements. The crystals were collected, washed with diethyl ether and *n*-pentane, and dried under vacuo. Compounds **2b** and **2c** were obtained in crystalline yields of 52 and 55%, respectively.

*Compound **2b**.* ^{1}H NMR (CD_3CN): δ 7.38−7.54 (m, 40H, H_{ph}), 5.26 (t, 4H, H_{cp}), 4.88 (t, 4H, H_{cp}), 4.34 (p, 4H, CH_2), 4.17 (s, 10H,

DOI: 10.1021/ic502913w
Inorg. Chem. 2015, 54, 3272−3280

H_{cp}). ^{11}B NMR (CD_3CN): δ −1.17 (s, BF_4^-). ^{13}C NMR (CD_3CN): δ 192.1 (COO^-), 134.2 (m, C_{ph}), 132.8 (m, C_{ph}), 130.1 (m, C_{ph}), 75.49 ($C_{quart\text{-}cp}$), 73.47 (C_{cp}), 72.07 (C_{cp}) 70.64 (C_{cp}), 37.40 (t, CH_2). ^{19}F NMR (CD_3CN): δ −151.69 (s, BF_4^-), −151.74 (s, BF_4^-). ^{31}P NMR (CD_3CN): δ18.69. Anal. Calcd for ($C_{72}H_{62}B_2F_8Fe_2Mo_2O_4P_4$) = $[Mo_2(O_2C\text{-}Fc)_2(DPPM)_2][BF_4]_2$: C, 54.31; H, 3.92; P, 7.78. Found: C, 54.29; H, 4.02; P, 7.67. Selected IR (cm^{-1}): ν_a(COO) 1484m, ν_s(COO) 1389m, ν(BF) 1093m, 1078m. ESI-MS (m/z): $[DPPM + H]^+$, 385.1 (calcd 385.1); $[(M - 2BF_4)/2]^+$, 709.1, 709.9, 710.8 (calcd 709.0, 709.5, 710.5); $[M - DPPM - 2BF_4 + HCOO]^+$, 1076.9, 1077.9, 1078.9, 1079.9, 1080.9 (calcd 1076.9, 1077.9, 1078.9, 1079.9, 1080.9).

Compound **2c**. ^1H NMR (CD_3CN): δ 7.58 (t, 8H, p-H_{ph}), 7.47 (t, 16H, o-H_{ph}), 7.33 (m, 16H, m-H_{ph}), 4.85 (t, 4H, H_{cp}), 4.72 (t, 4H, H_{cp}), 3.68 (s, 10H, H_{cp}), 2.86 (t, 8H, CH_2CH_2). ^{11}B NMR (CD_3CN): δ −1.18 (s, BF_4^-). ^{13}C NMR (CD_3CN): δ 190.9 (COO^-), 134.0 (m, C_{ph}), 133.0 (m, C_{ph}), 130.5 (m, C_{ph}), 73.75 ($C_{quart\text{-}cp}$), 73.65 (C_{cp}), 71.72 (C_{cp}), 70.64 (C_{cp}). ^{19}F NMR (CD_3CN): δ −151.73 (s, BF_4^-), −151.79 (s, BF_4^-). ^{31}P NMR (CD_3CN): δ 20.72. Anal. Calcd for ($C_{74}H_{66}B_2F_8Fe_2Mo_2O_4P_4$) = $[Mo_2(O_2C\text{-}Fc)_2(DPPE)_2][BF_4]_2$: C, 54.85; H, 4.11; P, 7.65. Found: C, 54.74; H, 4.14; P, 7.56. Selected IR (cm^{-1}): ν_a(COO) 1487m, ν_s(COO) 1390m, ν(BF) 1080m, 1072m. ESI-MS (m/z): $[DPPE + H]^+$, 399.2 (calcd 399.1); $[(M - 2BF_4)/2]^+$, 722.4, 723.4, 724.3 (calcd 723.0, 723.5, 724.0); $[M - DPPE - 2BF_4 + HCOO]^+$, 1092.9, 1093.9, 1094.9, 1095.8 (calcd 1092.9, 1093.9, 1094.9, 1095.9).

X-ray Structure Determination. Data were collected on a single-crystal X-ray diffractometer equipped with a CCD detector (Bruker APEX II, κ-CCD), a rotating anode (Bruker AXS, FR591) with Mo Kα radiation (λ = 0.71073 Å), a Montel optic (**2c**) or a fine-focused sealed tube with Mo Kα radiation (λ = 0.71073 Å), and a graphite monochromator (**2a** and **2b**) by using the *APEX2* software package.[60] The measurements were performed on a single crystal coated with perfluorinated ether. The crystal was fixed on top of a glass fiber and transferred to the diffractometer. The crystal was frozen under a stream of cold nitrogen. A matrix scan was used to determine the initial lattice parameters. Reflections were merged and corrected for Lorenz and polarization effects, scan speed, and background using *SAINT*.[61] Absorption corrections, including odd- and even-ordered spherical harmonics, were performed using *SADABS*.[61] Space-group assignments were based on systematic absences, E statistics, and successful refinement of the structures. Structures were solved by direct methods with the aid of successive difference Fourier maps and were refined against all data using *WinGX*[62] based on *SIR-92*[63] or *SHELXLE*[64] in conjunction with *SHELXL-97*.[65] Hydrogen atoms were assigned to ideal positions and refined using a riding model with an isotropic thermal parameter 1.2 times that of the attached carbon atom (1.5 times for methyl hydrogen atoms). If not mentioned otherwise, non-hydrogen atoms were refined with anisotropic displacement parameters. Full-matrix least-squares refinements were carried out by minimizing $\sum w(F_o^2 - F_c^2)^2$ with the *SHELXL-97*[65] weighting scheme. Neutral atom scattering factors for all atoms and anomalous dispersion corrections for the non-hydrogen atoms were taken from *International Tables for Crystallography*.[66] Images of the crystal structures were generated by *PLATON*.[67]

■ ASSOCIATED CONTENT

Supporting Information

XYZ coordinates, X-ray crystallographic data in CIF format, and listings of spectroscopic, crystallographic, and TG−MS data and computational details. This material is available free of charge via the Internet at http://pubs.acs.org. CCDC 1033919 (**2b**) and 1033920 (**2c**) contain the supplementary crystallographic data for this paper. These data can be obtained free of charge from The Cambridge Crystallographic Data Centre via www.ccdc.cam.ac.uk/data_request/cif.

■ AUTHOR INFORMATION

Corresponding Author

*E-mail: fritz.kuehn@ch.tum.de.

Author Contributions

†These authors contributed equally to this work.

Notes

The authors declare no competing financial interest.

■ ACKNOWLEDGMENTS

The TUM Graduate School and support from both the China Scholarship Council (Ph.D. grant to X.-M.C.) and the Fonds der Chemischen Industrie (Ph.D. grant to K.R.) are gratefully acknowledged. Additionally, we thank Dr. Markus Drees for helpful discussions and Master's student Wen-Qian Liang for experimental assistance.

■ REFERENCES

(1) Höhne, D.; Herdtweck, E.; Pöthig, A.; Kühn, F. E. *Dalton Trans.* **2014**, *43*, 15367−15374.

(2) Cai, X.-M.; Höhne, D.; Köberl, M.; Cokoja, M.; Pöthig, A.; Herdtweck, E.; Haslinger, S.; Herrmann, W. A.; Kühn, F. E. *Organometallics* **2013**, *32*, 6004−6011.

(3) Köberl, M.; Cokoja, M.; Bechlars, B.; Herdtweck, E.; Kühn, F. E. *Dalton Trans.* **2011**, *40*, 11490−11496.

(4) Köberl, M.; Cokoja, M.; Herrmann, W. A.; Kühn, F. E. *Dalton Trans.* **2011**, *40*, 6834−6859.

(5) Chisholm, M. H.; Patmore, N. J.; Reed, C. R.; Singh, N. *Inorg. Chem.* **2010**, *49*, 7116−7122.

(6) Majumdar, M.; Patra, S. K.; Kannan, M.; Dunbar, K. R.; Bera, J. K. *Inorg. Chem.* **2008**, *47*, 2212−2222.

(7) Cotton, F. A.; Murillo, C. A.; Yu, R.-M. *Dalton Trans.* **2006**, 3900−3905.

(8) Cotton, F. A.; Murillo, C. A.; Walton, R. A. *Multiple Bonds Between Metal Atoms*, 3rd ed.; Springer Science and Business Media Inc.; New York, 2005; pp 69−182.

(9) Cotton, F. A.; Lin, C.; Murillo, C. A. *Inorg. Chem.* **2004**, *43*, 2267−2276.

(10) Cotton, F. A.; Lin, C.; Murillo, C. A. *Proc. Natl. Acad. Sci. U. S. A.* **2002**, *99*, 4810−4813.

(11) Cotton, F. A.; Lin, C.; Murillo, C. A. *Inorg. Chem.* **2001**, *40*, 575−577.

(12) Cotton, F. A.; Lin, C.; Murillo, C. A. *Chem. Commun.* **2001**, 11−12.

(13) Fritsch, N.; Wick, C. R.; Waidmann, T.; Dral, P. O.; Tucher, J.; Heinemann, F. W.; Shubina, T. E.; Clark, T.; Burzlaff, N. *Inorg. Chem.* **2014**, *53*, 12305−12314.

(14) Wilkinson, L. A.; McNeil, L.; Scattergood, P. A.; Patmore, N. J. *Inorg. Chem.* **2013**, *52*, 9683−9691.

(15) Wilkinson, L. A.; McNeill, L.; Patmore, N. J. *J. Am. Chem. Soc.* **2013**, *135*, 1723−1726.

(16) Xiao, X.; Liu, C.-Y.; He, Q.; Lu, X. *Inorg. Chem.* **2013**, *52*, 12624−12633.

(17) Xi, B.; Liu, I. P.-C.; Xu, G.-L.; Choudhuri, M. M. R.; DeRosa, M. C.; Crutchley, R. J.; Ren, T. *J. Am. Chem. Soc.* **2011**, *133*, 15094−15104.

(18) Cotton, F. A.; Murillo, C. A.; Zhao, Q. *Inorg. Chem.* **2009**, *48*, 11755−11766.

(19) Cotton, F. A.; Li, Z.; Murillo, C. A. *Inorg. Chem.* **2009**, *48*, 11847−11852.

(20) Cotton, F. A.; Li, Z.; Liu, C.-Y.; Murillo, C. A. *Inorg. Chem.* **2007**, *46*, 7840−7847.

(21) Jeffery, S. P.; Darensbourg, M. Y. *Chem. Commun.* **2005**, 1122−1124.

(22) Ren, T. *Organometallics* **2005**, *24*, 4854−4870.

(23) Cotton, F. A.; Daniels, L. M.; Wikinson, C. C. *J. Am. Chem. Soc.* **2002**, *124*, 9249−9256.

DOI: 10.1021/ic502913w
Inorg. Chem. 2015, 54, 3272−3280

(24) Cotton, F. A.; Lin, C.; Murillo, C. A. *Inorg. Chem.* **2001**, *40*, 472−477.
(25) Cotton, F. A.; Lin, C.; Murillo, C. A. *J. Am. Chem. Soc.* **2001**, *123*, 2670−2671.
(26) Xue, W.-M.; Kühn, F. E. *Eur. J. Inorg. Chem.* **2001**, 2041−2047.
(27) Xue, W.-M.; Kühn, F. E.; Herdtweck, E.; Li, Q. *Eur. J. Inorg. Chem.* **2001**, 213−221.
(28) Cai, X.-M.; Zhang, X.-Y.; Savchenko, J.; Cao, Z.; Ren, T.; Zuo, J.-L. *Organometallics* **2012**, *31*, 8591−8597.
(29) Zhang, X.-Y.; Zheng, Q.; Qian, C.-X.; Zuo, J.-L. *Chin. J. Inorg. Chem.* **2011**, *27*, 1451−1464.
(30) Lorcy, D.; Bellec, N.; Fourmigue, M.; Avarvari, N. *Coord. Chem. Rev.* **2009**, *253*, 1398−1438.
(31) Chisholm, M. H.; Patmore, N. J. *Acc. Chem. Res.* **2007**, *40*, 19−27.
(32) Cao, Z.; Xi, B.; Jodoin, D. S.; Zhang, L.; Cummings, S. P.; Gao, Y.; Tyler, S. F.; Fanwick, P. E.; Crutchley, R. J.; Ren, T. *J. Am. Chem. Soc.* **2014**, *136*, 12174−12183.
(33) Zuo, J.-L.; Herdtweck, E.; Kühn, F. E. *J. Chem. Soc., Dalton Trans.* **2002**, 1244−1246.
(34) Cotton, F. A.; Lin, C.; Murillo, C. A. *Inorg. Chem.* **2001**, *40*, 478−484.
(35) Cotton, F. A.; Donahue, J. P.; Lin, C.; Murillo, C. A. *Inorg. Chem.* **2001**, *40*, 1234−1244.
(36) Cotton, F. A.; Daniels, L. M.; Lin, C.; Murillo, C. A. *J. Am. Chem. Soc.* **1999**, *121*, 4538−4539.
(37) Forrest, W. P.; Cao, Z.; Hassel, K. M.; Ren, T. *Inorg. Chem.* **2012**, *51*, 3261−3269.
(38) Boyd, D. A.; Fanwick, P. E.; Ren, T. *Inorg. Chim. Acta* **2011**, *370*, 198−202.
(39) Boyd, D. A.; Crutchley, R. J.; Fanwick, P. E.; Ren, T. *Inorg. Chem.* **2010**, *49*, 1322−1324.
(40) Boyd, D. A.; Cao, Z.; Song, Y.; Wang, T.-W.; Fanwick, P. E.; Crutchley, R. J.; Ren, T. *Inorg. Chem.* **2010**, *49*, 11525−11531.
(41) Xi, B.; Xu, G.-L.; Fanwick, P. E.; Ren, T. *Organometallics* **2009**, *28*, 2338−2341.
(42) Fan, Y.; Po, I.; Liu, C.; Ren, T. *Organometallics* **2009**, *28*, 3959−3962.
(43) Xu, G.-L.; Crutchley, R. J.; DeRosa, M. C.; Pan, Q.-J.; Ren, T. *J. Am. Chem. Soc.* **2005**, *127*, 13354−13363.
(44) Xi, G.-L.; DeRosa, M. C.; Crutchley, R. J.; Ren, T. *J. Am. Chem. Soc.* **2004**, *126*, 3728−3729.
(45) Brown-Xu, S. E.; Chisholm, M. H.; Durr, C. B.; Lewis, S. A.; Spilker, T. F.; Young, P. J. *Chem. Sci.* **2014**, *5*, 2657−2666.
(46) Bunting, P.; Chisholm, M. H.; Gallucci, J. C.; Lear, B. J. *J. Am. Chem. Soc.* **2011**, *133*, 5873−5881.
(47) Brown, D. J.; Chisholm, M. H.; Gallucci, J. C. *Dalton Trans.* **2008**, 1615−1624.
(48) Arnold, D. I.; Cotton, F. A.; Kühn, F. E. *Inorg. Chem.* **1996**, *35*, 5764−5769.
(49) Arnold, D. I.; Cotton, F. A.; Kühn, F. E. *Inorg. Chem.* **1996**, *35*, 4733−4737.
(50) Cotton, F. A.; Kühn, F. E. *Inorg. Chim. Acta* **1996**, *252*, 257−264.
(51) Farrugis, L. J.; McVitie, A.; Peacock, R. D. *Inorg. Chem.* **1988**, *27*, 1257−1260.
(52) Xue, W.-M.; Kühn, F. E.; Zhang, G.-F.; Herdtweck, E.; Raudaschl-Sieber, G. *J. Chem. Soc., Dalton Trans.* **1999**, 4103−4110.
(53) Cotton, F. A.; Daniels, L. M.; Haefner, S. C.; Kühn, F. E. *Inorg. Chim. Acta* **1999**, *287*, 159−166.
(54) Armarego, W. L. F.; Chai, C. *Purification of Laboratory Chemicals*; Elsevier Science: New York, 2009; pp 25−30.
(55) Frisch, M. J.; Trucks, G. W.; Schlegel, H. B.; Scuseria, G. E.; Robb, M. A.; Cheeseman, J. R.; Scalmani, G.; Barone, V.; Mennucci, B.; Petersson, G. A.; Nakatsuji, H.; Caricato, M.; Li, X.; Hratchian, H. P.; Izmaylov, A. F.; Bloino, J.; Zheng, G.; Sonnenberg, J. L.; Hada, M.; Ehara, M.; Toyota, K.; Fukuda, R.; Hasegawa, J.; Ishida, M.; Nakajima, T.; Honda, Y.; Kitao, O.; Nakai, H.; Vreven, T.; Montgomery, J. A., Jr.; Peralta, J. E.; Ogliaro, F.; Bearpark, M. J.; Heyd, J.; Brothers, E. N.; Kudin, K. N.; Staroverov, V. N.; Kobayashi, R.; Normand, J.; Raghavachari, K.; Rendell, A. P.; Burant, J. C.; Iyengar, S. S.; Tomasi, J.; Cossi, M.; Rega, N.; Millam, N. J.; Klene, M.; Knox, J. E.; Cross, J. B.; Bakken, V.; Adamo, C.; Jaramillo, J.; Gomperts, R.; Stratmann, R. E.; Yazyev, O.; Austin, A. J.; Cammi, R.; Pomelli, C.; Ochterski, J. W.; Martin, R. L.; Morokuma, K.; Zakrzewski, V. G.; Voth, G. A.; Salvador, P.; Dannenberg, J. J.; Dapprich, S.; Daniels, A. D.; Farkas, Ö.; Foresman, J. B.; Ortiz, J. V.; Cioslowski, J.; Fox, D. J. *Gaussian09*; Gaussian, Inc.: Wallingford, CT, 2009.
(56) Cohen, A. J.; Handy, N. C. *Mol. Phys.* **2001**, *99*, 607−615.
(57) Lee, C.; Yang, W.; Parr, R. G. *Phys. Rev. B* **1988**, *37*, 785−789.
(58) Hehre, W. J.; Ditchfield, R.; Pople, J. A. *J. Chem. Phys.* **1972**, *56*, 2257−2261.
(59) Francl, M. M.; Pietro, W. J.; Hehre, W. J.; Binkley, J. S.; Gordon, M. S.; DeFrees, D. J.; Pople, J. A. *J. Chem. Phys.* **1982**, *77*, 3654−3665.
(60) *APEX Suite of Crystallographic Software, APEX 2*, version 2008.4; Bruker AXS Inc.: Madison, WI, 2008.
(61) *SAINT*, version 7.56a; *SADABS*, version 2008.1; Bruker AXS Inc.: Madison, WI, 2008.
(62) Farrugia, L. J. *J. Appl. Crystallogr.* **1999**, *32*, 837−838.
(63) Altomare, A.; Cascarano, G.; Giacovazzo, C.; Guagliardi, A.; Burla, M. C.; Polidori, G.; M, C. *J. Appl. Crystallogr.* **1994**, *27*, 435−436.
(64) SHELXLE: Huebschle, C. B.; Sheldrick, G. M.; Dittrich, B. *J. Appl. Crystallogr.* **2011**, *44*, 1281−1284.
(65) Sheldrick, G. M. *SHELXL-97*; University of Göttingen: Göttingen, Germany, 1998.
(66) Wilson, A. J. C. *International Tables for Crystallography*; Kluwer Academic Publishers: Dordrecht, The Netherlands, 1992.
(67) Spek, A. L. *PLATON, A Multipurpose Crystallographic Tool*; Utrecht University: Utrecht, The Netherlands, 2010.

DOI: 10.1021/ic502913w
Inorg. Chem. 2015, 54, 3272−3280